A Phosphotungstic Acid Catalyst for Depolymerization in Bulrush Lignin

Boyu Du [1], Bingyang Liu [1], Yingying Yang [1], Xing Wang [1,2,3,*] and Jinghui Zhou [1,*]

1   Liaoning Key Laboratory of Pulp and Papermaking Engineering, Dalian Polytechnic University, Dalian 116034, Liaoning, China; duboyu0501@163.com (B.D.); liubingyang303@163.com (B.L.); yangyingying@yeah.net (Y.Y.)
2   Guangxi Key Laboratory of Clean Pulp & Papermaking and Pollution Control, College of Light Industry and Food Engineering, Guangxi University, Nanning 530004, China
3   State Key Laboratory of Pulp and Paper Engineering, South China University of Technology, Guangzhou 510640, China
*   Correspondence: wangxing@dlpu.edu.cn (X.W.); zhoujh@dlpu.edu.cn (J.Z.); Tel.: +86-411-8632-3296 (X.W.)

check for updates

Abstract: Obtaining renewable fuels and chemicals from lignin is an important challenge in the use of biomass to achieve sustainability and energy goals. At present, acid-based catalysts for lignin depolymerization are considered to be a potential but challenging way to produce low-molecular-mass aromatic chemicals. The main concerns with the use of Lewis acids and zeolite catalysts are the corrosive nature of the acids, the possible formation of unwanted byproducts, and the possible formation of harsh reaction conditions. We achieved high-yield conversion using phosphotungstic acid (PTA) polyoxometalate catalysts in ethanol/water under different reaction conditions with little formation of bio-char. The monomeric products were mainly composed of various types of aromatic compounds. Our method does not require the use of precious metals and harsh reaction conditions—it only requires relatively mild reaction conditions and homogeneous catalysis—thereby greatly reducing operating costs and increasing the yields. Therefore, this PTA catalyst, which has excellent performance in bulrush lignin catalysis, would be a good alternative to the traditional catalysts used in lignin depolymerization and have wide application in biomass use.

Keywords: lignin; catalytic depolymerization; phosphotungstic acid catalyst; β-O-4

1. Introduction

The development of industry and growth of the world's population have increased the global consumption of fossil fuels and related environmental problems. Finding sustainable resources for use as new energy sources and materials remains a challenge [1]. Biomass is considered to be the only sustainable alternative to fossil fuels for the production of value-added chemicals [2]. Lignin is the second largest source of biomass on Earth, and, compared to cellulose and hemicellulose, is the most abundant natural source of non-fossil-based aromatic hydrocarbons, due to having high carbon content and high thermal stability [3]. It represents a sustainable natural resource and is a phenolic polymer derived primarily from three hydroxycinnamyl alcohols: p-coumaryl alcohol, coniferyl alcohol, and sinapyl alcohol [4]. The presence of these advantages and functional groups suggests that lignin has great potential in the production of renewable aromatic platform chemicals and carbon materials.

During the pulping process, the amount of produced lignin residue exceeds 50 million tons per year [5]. Lignin is also a byproduct of the production of second-generation ethanol fuel from crop waste [6]. These processes can produce large amounts of lignin feedstock. Based on lignin's high yields and diverse chemical groups, recent studies have shown that lignin can be an effective source of

biofuel and specialty chemicals such as phenolic monomers, including phenols, guaiacols, syringol, and catechols [7]. It is well-known that these "green chemicals" can be used as food additives and biopreservatives; pharmaceutical products; industrial products for resin, plastic, and composites' manufacture; as well as commodity product (conversion biofuel) by catalytic depolymerization [4,8]. Recent studies on the catalytic depolymerization conversion of lignin have shown that it can be converted into various monomers [8]. The focus of most of the previous literature is on obtaining higher yields by carrying out catalytic oxidation in a suitable solvent, such as water [9], ethanol [10], methanol [11], and water/ethanol [12]. Among the investigated solvents, ethanol produced the best results [13]. According to this result, we further found that the use of a suitable catalyst to promote lignin depolymerization is an attractive strategy to achieve high yields of, and high selectivity for, desired phenolic products. Renders et al. [14] reported that on the different influence of acidic (H_3PO_4) and alkaline (NaOH) additives on the Pd/C-catalyzed reductive processing of poplar wood in methanol (MeOH). It was found that the addition of small quantities of H_3PO_4 results in three rather than two product streams and according to this new efficiency measure, mildly acidic conditions performed best. Yang et al. [15] proposed a high-temperature heterogeneous acid catalytic depolymerization process. HZSM-5 zeolite catalysts can promote the formation of aromatic hydrocarbons, such as phenol, guaiacol, and syringol, during lignin pyrolysis. Besides this, heteropoly acid polyoxometalates are considered to be environmentally benign and economically feasible solid acid catalysts due to their excellent functional characteristics, such as ease of handling and removal; reusability; low number of side reactions; strong Bronsted acidity (approaching the super-acid region); and high proton mobility, stability, and catalytic activity [16,17]. Voitl et al. [16] studied the use of polyoxometalates as reversible oxidants and radical scavengers, which prevent lignin fragments from repolymerizing. Vanillin and methyl vanillate were the main obtained products. Deng et al. [17] reported that several vanadium-substituted Keggin-type polyoxometalates show firm acidity and catalyze the conversion of cornstalk lignin to low-molecular-weight aromatics. Xu et al. [18] explored the catalytic performance of oxidative depolymerization of enzymatically hydrolyzed lignin from a cellulosic ethanol fermentation residue by different vanadium-substituted Keggin-type polyoxometalates ($K_5[SiVW_{11}O_{40}]$, $K_6[SiV_2W_{10}O_{40}]$, and $K_6H[SiV_3W_9O_{40}]$). The best result, with respect to lignin conversion and lignin oil production, was obtained by $K_6[SiV_2W_{10}O_{40}]$, which produced the highest yield of oxidative depolymerization products (53%). Nevertheless, the main concerns with the use of Bronsted and Lewis acid catalysts are the corrosive nature of the acids, the possible formation of excess byproducts, the possible formation of harsh reaction conditions, and the requirement for polyoxometalate catalysts [15,16,19].

The present work aims at a phosphotungstic acid (PTA) polyoxometallate catalyst that can efficiently and homogeneously convert bulrush lignin in ethanol/water. Our goal is to address the disadvantages of using acid catalysts for lignin depolymerization into phenolic monomers. Bulrush lignin depolymerization for preparing monophenol compounds was studied using Fourier transform infrared spectroscopy (FT–IR), gel permeation chromatography (GPC), thermal analyzer (TGA), elemental analysis, gas chromatography–mass spectrometry (GC–MS), gas chromatography–flame ionization detector (GC–FID), and two-dimensional (2D) heteronuclear single quantum coherence nuclear magnetic resonance (2D-HSQC NMR). The results from this study indicate that the PTA catalyst would provide a viable option for the production of aromatic monomers from lignin under different reaction conditions.

2. Results and Discussion

2.1. Characterization of the Bulrush Lignin

Chemical analysis with FT–IR, TGA, GPC, elemental analysis, and 2D-HSQC NMR revealed the bulrush lignin's FT–IR spectrum, thermal stability, mass-average molecular weight (Mw), H/C and O/C, and changes in chemical linkage frequencies.

2D-HSQC NMR, which is generally employed to elucidate a lignin's structure, was used to characterize the BL. 2D-HSQC NMR for identifying structures is based on their chemical shifts [20,21]. Figure 1 shows the 2D-HSQC NMR spectra of the internal linkages within bulrush lignin (BL) before PTA catalytic depolymerization. They consist of two regions: the aliphatic region (δC/δH 49–91/2.4–5.8 ppm) and the aromatic region (δC/δH 79–135/5.7–7.9 ppm). The amounts of H, G, and S units observed in the aromatic region were 36.2%, 33.6%, and 30.2%, respectively, suggesting that the BL is a typical SGH-type (including H, G, and S units) grass lignin [4]. In the aliphatic regions (δC/δH 49–91/2.4–5.8 ppm) of the 2D-HSQC NMR, cross-signals of methoxy groups (OMe), β-O-4 aryl ether linkages (A), β-β linkages (B), and β-5 linkages (C) were all recognizable. On the other hand, the corresponding correlations of β-D-xylopyranoside units (X_2, X_3, and X_4) were tested for the BL and demonstrate the existence of carbohydrate structures in these lignin samples. A quantitative content analysis of internal linkages (β-O-4, β-β, and β-5) and aromatic units was performed using the procedure described in [20], and the results are illustrated in Figure 1. The maximum content of β-O-4 bonds in the BL is 26.1/100 Ar. The maximum content of β-β linkages and β-5 linkages in the BL is 3.8/100 Ar and 5.1/100 Ar, respectively. It has been reported that there are more C-O linkages (mostly β-O-4 aryl ether bonds) and C-C structures in lignin, which are relatively more straightforward to depolymerize [22]. Thus, BL, with its higher β-O-4 content, might be a better raw material for depolymerization, which provides a platform for the production of aromatic compounds.

Figure 2a displays the FT–IR spectra of the BL. The band assignments are based on reported data [23]. As can be seen from the spectrum of the BL, a wide absorption band appeared at 3400 cm^{-1}, which was assigned to phenolic or aliphatic OH groups. The bands at 2939 cm^{-1} and 2844 cm^{-1} were assigned to the asymmetric and symmetrical vibrations of the methyl and methylene groups of C-H, respectively. The peak was associated with the C=O stretching vibrations in the conjugated carboxylic acid at 1680 cm^{-1}. The bands observed at 1600, 1517, and 1461 cm^{-1} were assigned to an aromatic ring stretching mode of the phenyl-propane skeleton, indicating that the BL extract shares the basic skeleton of lignin. The C=O vibration band in the conjugated ester groups at 1166 cm^{-1} and the C-H out-of-plane vibrations at 839 cm^{-1} indicate that bulrush lignin is a GSH-type grass lignin [4]. The TGA result is shown in Figure 2b. The lignin's decomposition process is divided into three parts. In the first part, moisture loss in the lignin occurs at 100 °C. The second part (from 200 °C to 400 °C) is caused by a loss of side chain lignin mass and the breaking of the β-O-4 aryl ether bond. The third part (beyond 400 °C) is due to the decomposition of lignin, mainly C_5–C_5 breakages and cracking of the aromatic ring to remove methoxy. Finally, lignin degradation almost stops at 700 °C. The BL production rate after complete thermal degradation is 39.2%. At this time, the main β-O-4 ether bond is broken. The thermal stability of lignin is greatly affected by the β-O-4 ether bond. As an important thermodynamic property of lignin, it is known that lignin is also affected by the degree of lignin condensation and hydroxyl content, and the specific reasons for this need to be further explored [24]. GPC was performed to analyze the molecular weight distributions of the lignin from bulrush pulping and ethanol extraction. The results show that the distribution curve of molecular weight exists in the high-molecular-weight area with underpolymerized bulrush lignin (BL). Meanwhile, the BL contains both small and large molecular weight lignin fragments. In order to quantitatively assess the BL, Figure 2c illustrates the weight-average molecular weight (Mw), number-average molecular weight (Mn), and polydispersity index (PDI). As expected, the BL has a relatively high molecular weight (4371 g/mol (Mw)) and polydispersity (4.02). Figure 2d depicts the H/C and O/C atomic ratios of the BL obtained after ethanol/water extraction at 205 °C. These results indicate that the BL may contain more oxygen functional groups, such as aryl ether linkages and methoxyl [25].
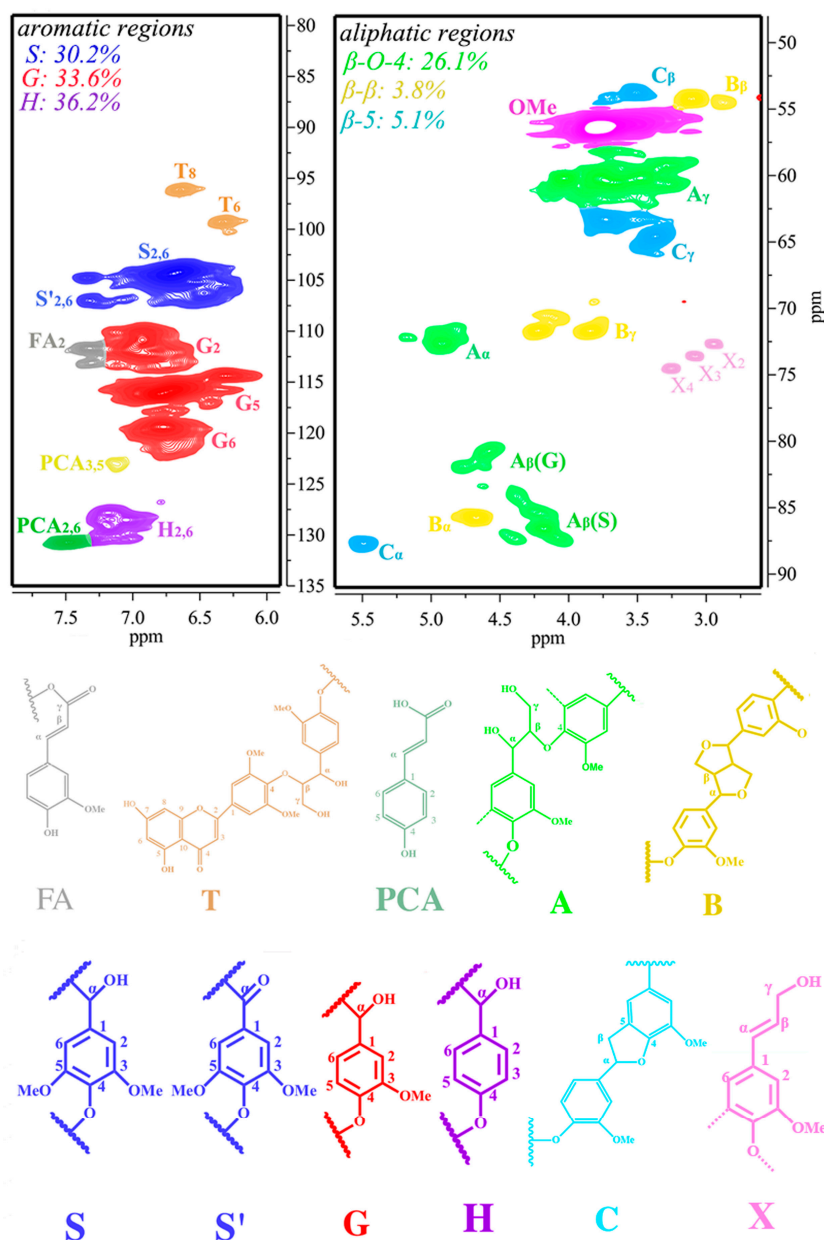
Figure 1. The two-dimensional heteronuclear single quantum coherence nuclear magnetic resonance (2D-HSQC NMR) spectra of the bulrush lignin (BL).

2.2. Catalysis of the Bulrush Lignin and β-O-4 Model Compound by PTA Catalyst

In order to explore the potential of PTA for the catalysis of β-O-4 linkages in lignin, depolymerization of the BL with PTA catalyst was performed in ethanol/water under different reaction conditions. Table 1 summarizes the results of different catalysts on the depolymerization of bulrush lignin. Conventional GC–MS and GC–FID were used to analyze the phenolic monomers. We developed a comprehensive workup procedure to differentiate phenols, oligomers (ethanol-soluble, EL), polymers (tetrahydrofuran (THF)-soluble, TL), and bio-char (THF-insoluble).
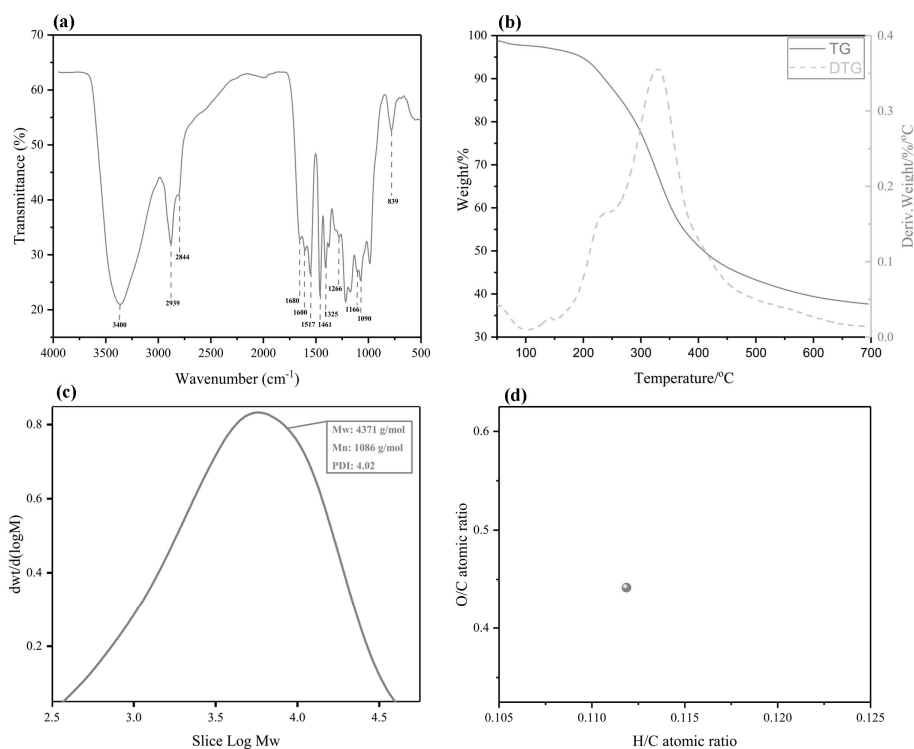
Figure 2. The Fourier transform infrared spectroscopy (FT–IR) spectra, TGA, gel permeation chromatography (GPC), and elemental analysis of the BL. (**a**) The FT–IR spectra; (**b**) the TGA; (**c**) the GPC; and (**d**) the elemental analysis.

Table 1. The mass balance of catalytic depolymerization products under different reaction conditions.

Entry	Catalyst	Temperature (°C)	Time (h)	Monomers (wt %)	EL-Soluble (wt %)	Tetrahydrofuran (THF)-Soluble (wt %)	Bio-Char (wt %)	Mass Balance (wt %)
1	None	250	6	0	17.24	30.39	44.41	92.04
2	AlCl₃	250	6	1.92	22.59 (250.6 EL)	39.58 (250.6 TL)	25.07	89.16
3	FeCl₂	250	6	1.79	23.35 (250.6 EL)	36.36 (250.6 TL)	27.69	89.19
4	HZSM-5	250	6	2.23	31.73 (250.6 EL)	36.72 (250.6 TL)	20.51	91.19
5	PTA	200	6	9.57	50.49 (200.6 EL)	32.53 (200.6 TL)	3.06	95.65
6	PTA	225	6	10.02	51.68 (225.6 EL)	31.71 (225.6 TL)	2.53	95.94
7	PTA	250	6	12.11	53.83 (250.6 EL)/(6 h EL)	31.59 (250.6 TL)/(6 h TL)	2.01	97.53
8	PTA	275	6	10.49	52.49 (275.6 EL)	32.64 (275.6 TL)	2.14	97.76
9	PTA	300	6	9.08	51.53 (300.6 EL)	34.57 (300.6 TL)	3.96	99.14
10	PTA	250	0.5	4.23	50.77 (0.5 h EL)	34.45 (0.5 h TL)	5.86	95.31
11	PTA	250	2	6.71	50.58 (2 h EL)	35.77 (2 h TL)	3.53	96.59
12	PTA	250	4	7.92	53.23 (4 h EL)	32.42 (4 h TL)	3.08	96.65
13	PTA	250	8	10.33	50.02 (8 h EL)	34.71 (8 h TL)	3.96	99.02

A blank test showed that lignin is depolymerized at 250 °C for 6 h without a catalyst (Table 1, entry 1). Most of it is converted to char and polymers (TL), yielding only 17.24% oligomers (EL), which are considered to be inefficient for biofuel production. Under the same reaction conditions

(250 °C, 6 h), the Lewis acids $AlCl_3$ and $FeCl_2$ facilitate the cleavage of ether bond, so 89.16% and 89.19% BL conversion, respectively, were obtained. However, the phenolic monomer yield still needs to be improved and the bio-char yield should be decreased (250 °C, 6 h, Table 1, entry 2 versus 3). According to a previous report, the reaction conditions for Lewis acids ($AlCl_3$ and $FeCl_2$) are harsh, such as a reaction temperature and time of 400 °C and 4 h, respectively. The yields of phenolic monomers obtained were 6.2% and 6.9%, respectively [26]. Compared with Lewis acid-based catalytic depolymerization, HZSM-5-zeolite-based catalytic depolymerization shows similar performance on both phenolic monomer formation and lignin conversion in this study. For example, when the HZSM-5 zeolite catalyst is used in the depolymerization reaction, the phenolic monomer yield is 2.23%, and the lignin conversion yield is 91.19% (250 °C, 6 h, Table 1, entry 4). Wang et al. [27] used HZSM-5 zeolites with different particle sizes as catalysts to depolymerize poplar lignin at a high temperature (350 °C), and they obtained a phenolic monomer yield of 11.2% with nano-HZSM-5 zeolite. However, an interesting finding is that PTA catalysts display high catalytic efficiency on phenolic monomer formation and bio-char elimination compared to HZSM-5-zeolite-based and Lewis acid-based catalytic depolymerization at the reaction temperature of 250 °C and the reaction time of 5 h (Table 1, entry 7). This result demonstrates PTA's excellent lignin depolymerization efficiency, which is based on its having a significant effect on the lignin product conversion. Then, we changed the reaction temperature and time to determine the optimal conditions for PTA-based catalytic depolymerization (Table 1, entries 5–13). A temperature increase from 200 °C to 300 °C under the same reaction time (6 h) yielded the maximum lignin conversion, and TL yield was 99.14% and 34.57%. The total relative yield of EL achieved a maximum of 53.83% at 250 °C. The reason for this phenomenon may be that the conversion products are further catalytically depolymerized at a suitable temperature and a condensation reaction tends to occur at a higher temperature [28,29]. Secondly, the conversion of lignin was carried out under different reaction time conditions. With respect to the ethanol solvent BL samples obtained under different reaction time conditions, the yield of EL reached a maximum at 6 h (53.83%). However, the 8 h reaction time BL samples obtained the highest yields of lignin conversion (99.02%) and TL (34.71%). Zhao et al. discovered that the phosphovanadomolybdate's ($H_5PMo_{10}V_2O_{40}$) catalysis reaction time affects the properties of catalysts after depolymerization [30]. In this study, the phenomenon may be due to the fact that the PTA catalysts have suitable catalysis activity for the depolymerization of the β-O-4 aryl ether bonds. A suitable reaction time can produce a large amount of phenolic monomers. As the reaction time increased, a remarkable increase in TL and char yields was observed, which can be attributed to the phenolic monomer and EL repolymerization. These results were also confirmed by analyzing the EL and TL using GPC and elemental analysis. Therefore, the PTA catalyst is an effective homogeneous catalyst and produces a good yield in catalyzing lignin under relatively mild conditions. In particular, compared with other reaction temperatures and times, a suitable condition (250 °C, 6 h) shows better performance for phenolic monomer formation.

In order to explore the effect of the PTA catalyst on lignin depolymerization, the lignin model compound and BL samples were used as substrates to verify the potential of PTA for the depolymerization of β-O-4 bonds. The monomer products were extracted by ethyl acetate and analyzed by GC–MS. The depolymerization products were identified by comparing their GC–MS retention times and mass spectra. In Figure 3, no starting dimer can be detected in the products of the dimer catalyzed by PTA, indicating that one kind of lignin model dimer is converted completely. As shown in Figure 3a, the lignin model is veratrylglycerol-β-guaiacyl ether (VG). Two main products were found at the retention times of 13 and 28 min. Among these monomer products, the 2-methoxyphenol (124) and 2-(4-hydroxy-3-methoxyphenyl)-acetaldehyde (166) compounds both have representative meanings. The reaction route of VG is shown in Figure 3b. The abstraction of the β-proton by a certain base affords the significantly acid labile enol ether compound 1-(2-methoxyphenoxy)-2-(3,4-dimethoxyphenyl) ethene (EE), which cannot be detected under general acidolysis conditions. EE is consecutively acid hydrolyzed at the β-O-4 bond to give 124 and 166 [31,32]. Thus, these results indicate the complete

cleavage of β-O-4 aryl ether bonds in the dimer after the catalysis of the β-O-4 lignin model dimer by the PTA catalyst.
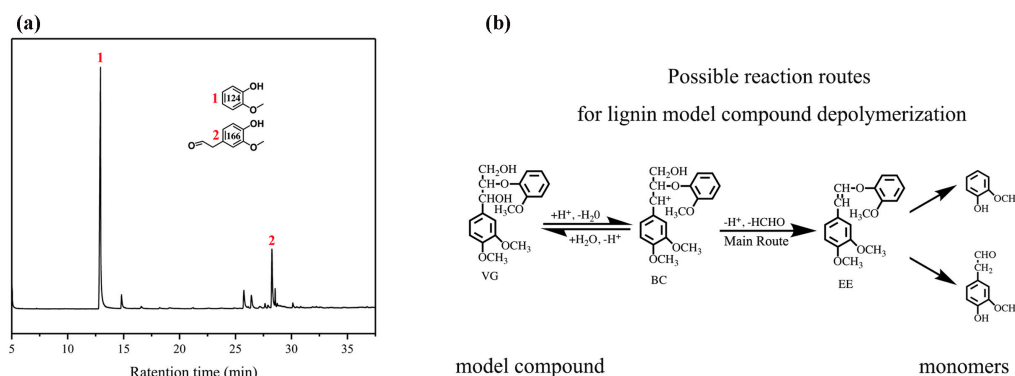

Figure 3. Phosphotungstic acid (PTA) catalytic depolymerization of the lignin model compound. (**a**) A gas chromatogram of the veratrylglycerol-β-guaiacyl ether under the PTA catalyst; (**b**) possible reaction routes for the veratrylglycerol-β-guaiacyl ether's depolymerization.

With respect to the treatment of BL with the PTA catalyst in a mixture of ethanol/water in an autoclave, a mixture solution was obtained. After acidification, the products were extracted with ethyl acetate. The amount of phenolic monomer that was obtained under the different reaction conditions, which was measured by GC–MS and GC–FID, is detailed in Figure 4. The composition of the depolymerized product did not change regardless of the used temperature. However, the reaction temperature had an influence on the content of each monophenol compound. As the temperature increased, the monophenols yield first increased and then decreased, reaching a maximum of 12.11% at 250 °C (Figure 4a). Figure 4b shows that the reaction time has an influence on the composition of each monophenols compound. As the reaction time increased, the yields of monophenols increased to a maximum of 12.11% at 6 h.
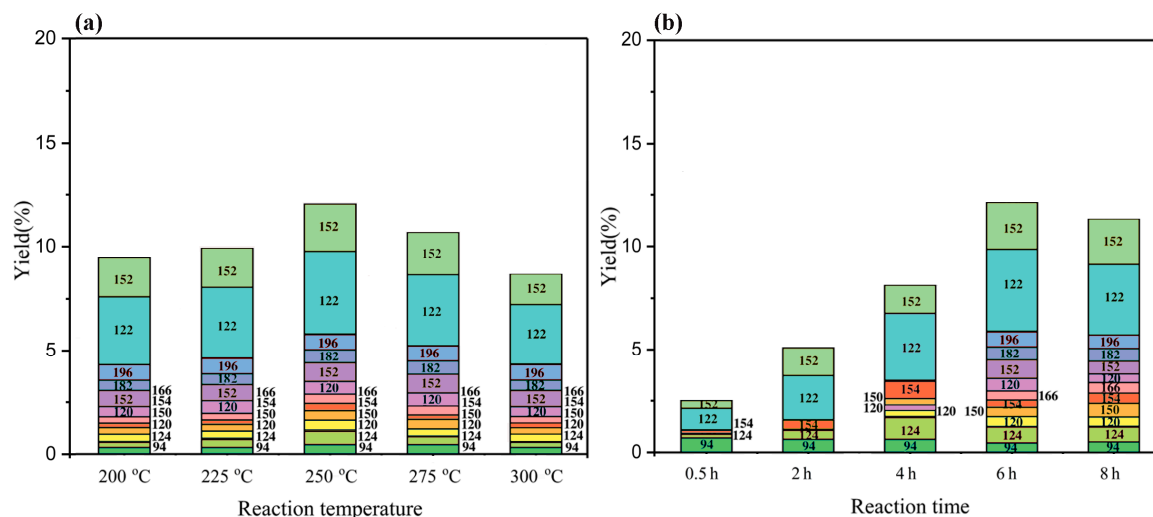

Figure 4. The monomeric yield distribution following the BL reaction under different reaction conditions. (**a**) The monomeric yield distribution following the BL reaction at different reaction temperatures for 6 h; (**b**) the monomeric yield distribution following the BL reaction at different reaction times for 250 °C.

The phenolic monomers are composed of less than thirteen kinds of compounds, including p-hydroxyphenyl, guaiacol, syringol, and their derivates, and a small number of other aromatic chemicals. The structure of these products is shown in Figure 5. Small molecule compounds obtained from the BL retain their aromatic character and aromatic hydroxyl groups, and these monomers fall

into three categories according to their aromatic rings (p-hydroxyphenyl, guaiacyl, and syringyl): H1~H4, G1~G5, and S1~S3. Because H_2O_2 was added to all reactions, some oxygenated phenolic monomers were produced. A dramatic change in H-type, G-type, and S-type yields were observed with the change in reaction conditions. These results show a significant promotion of H-type and G-type phenolic monomer yields, and a smaller S-type yield, with a change in reaction conditions (Figure 6). Taking temperature conditions as an example, the H-type and G-type yields can be promoted from 35.83% and 44.18% to 40.89% and 49.02%, respectively, by increasing the reaction temperature from 200 °C to 250 °C, with a decrease in the S-type yield from 19.19% to 10.09%. However, with a further increase in temperature, a remarkable decrease in the H-type and G-type yields was exhibited, which can be attributed to the oligomer repolymerization and demethoxylation reactions [33]. In the current work, the production of various phenolic monomers at a monomer yield of approximately 12.11% has been achieved. It is worth noting that phenolic monomer products produced by this PTA catalyst system have great potential to be a promising renewable alternative to fossil resources [34].
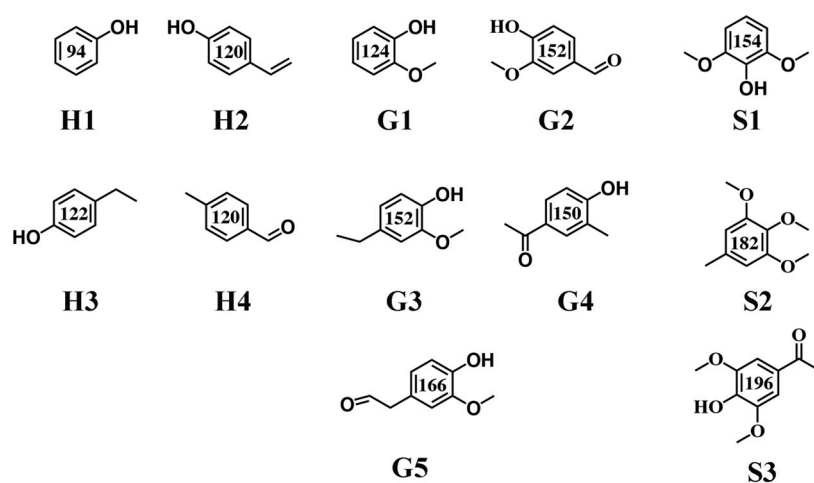

Figure 5. A summary of the monomer products obtained from the catalytic depolymerization of BL.
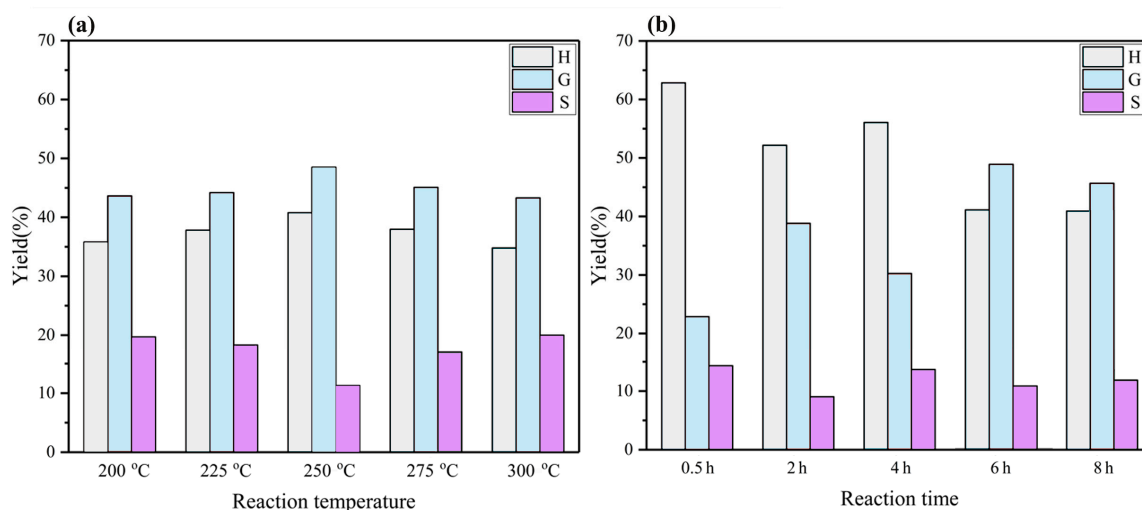

Figure 6. The SGH-type distribution of phenolic monomers. (**a**) The SGH-type distribution at different reaction temperatures; (**b**) the SGH-type distribution at different reaction times.

We also analyzed the phenolic products' structures by 2D-HSQC NMR spectrometry (Figure 7). The reaction temperature and time were 250 °C and 6 h, respectively. The 2D-HSQC NMR spectrum contains many cross-peaks assigned to phenolic products. It confirms our claim that PTA can effectively depolymerize lignin. As expected, the signals of Aα (δC/δH 71.5/4.82 ppm) and Aβ (δC/δH

83.6/4.43 ppm and 86.7/4.04 ppm), corresponding to benzylic alcohols and secondary alkyl protons of β-O-4 linkages, respectively, almost completely disappeared (Figures 1 and 8) in comparison to primitive lignin and residual lignin. Secondly, an obvious methoxy and aromatic ring structure was observed: OMe (δC/δH at 56.1/3.69), C$_2$ (δC/δH at 112.3/6.73), and C$_3$ (δC/δH at 112.8/6.86). This methoxy and aromatic ring structure arises from the catalytic depolymerization of bulrush lignin to form a large number of H-type, G-type, and S-type structural units [35]. Similarly, Figure 7 also shows that many other cross-peaks assigned to higher alcohol and alkyl ester aromatic products were formed (δC/δH at 119.3/6.76, δC/δH at 120.2/6.59, and δC/δH at 121.5/6.83). These results point out the fact that Guerbet reactions as well as esterification reactions of phenol were dominant in the PTA-based catalytic depolymerization reaction [36]. Thus, these 2D-HSQC NMR results also confirm the GC–MS analysis. In our study, lignin can be effectively depolymerized into different phenolic products by PTA polyoxometalates.
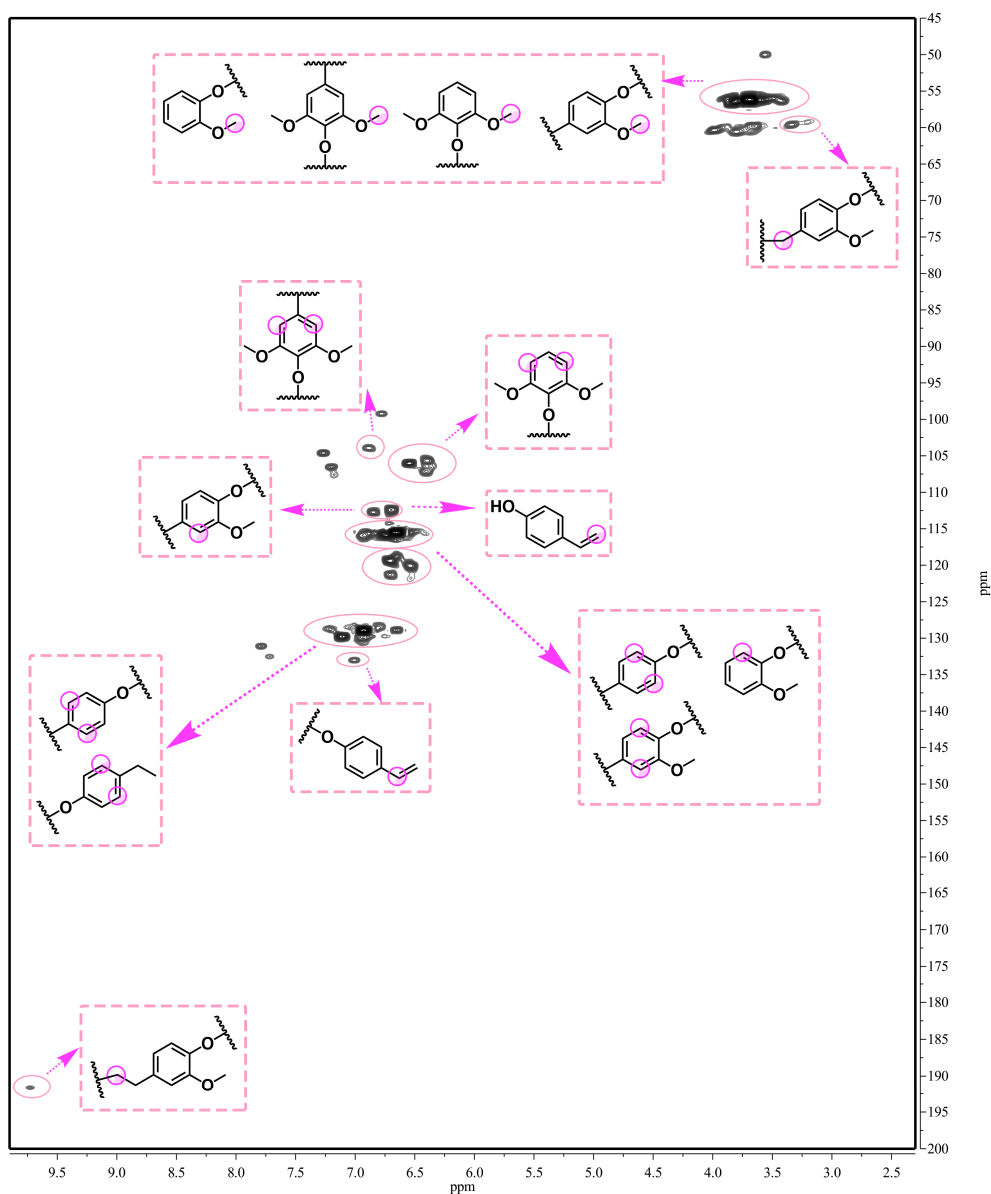

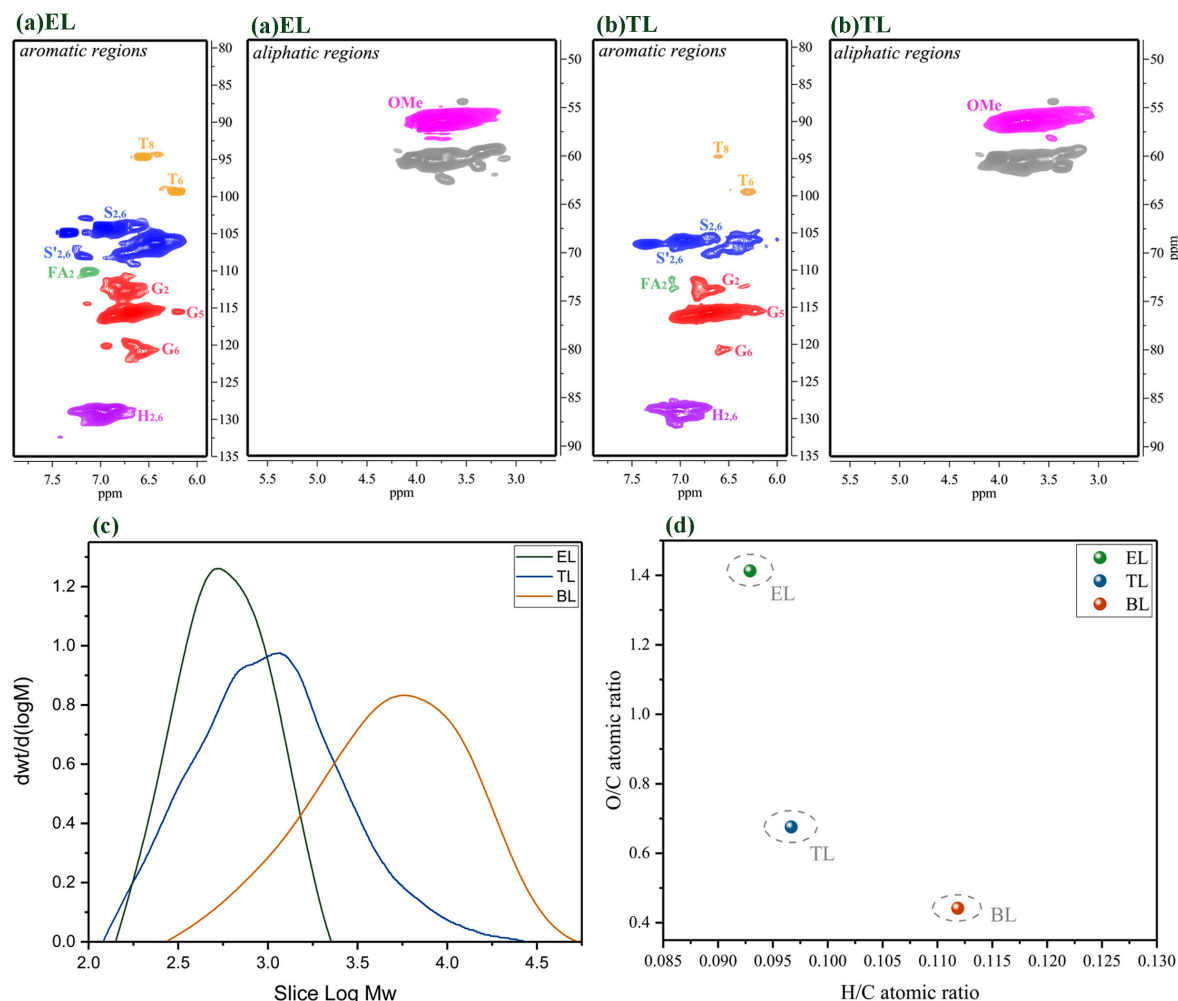**Figure 7.** The 2D-HSQC NMR spectra of the phenolic products (250 °C, 6 h).

Figure 8. The 2D-HSQC NMR spectra, GPC, and elemental analysis of the residual lignin at 250 °C for 6 h. (**a**) The 2D-HSQC NMR spectra of the ethanol-soluble (EL) residue at 250 °C for 6 h; (**b**) the 2D-HSQC NMR spectra of the THF-soluble (TL) residue at 250 °C for 6 h; (**c**) the GPC of the EL and TL residues at 250 °C for 6 h; (**d**) elemental analysis of the EL and TL residues at 250 °C for 6 h.

2.3. Characterization of the Residual Lignin

To compare the properties of residual lignin samples with different preparation principles, taking the 250 °C reaction temperature and 6 h reaction time as an example, residual lignin samples were analyzed by 2D-HSQC NMR, GPC, and elemental analysis.

As compared with the BL, the primary signals corresponding to the β-O-4 substructures had almost disappeared in the spectra of the lignin residue obtained under these reaction conditions and with PTA as a catalyst, implying extensive depolymerization and removal of the β-O-4 aryl ether bonds (Figure 8a,b). Previous studies have demonstrated that the β-ether and α-ether bonds in the β-O-4 and α-O-4 linkages in lignin are easily cleaved at a high temperature, while the aromatic ring structures are relatively stable [37]. In our research, in the presence of the PTA catalyst, lignin was degraded mostly into oligomers and monomers in the depolymerization process, and accompanied by condensation reactions. These results support the finding discussed above that the majority of lignin depolymerization products are phenolic monomers and small molecule lignin samples, and the depolymerization process is accompanied by repolymerization. The EL and TL lignin residues have only a faint signal of $C_{2,6}$–$H_{2,6}$ in the S and S' units during depolymerization with PTA as a catalyst. The molecular weight of the EL and TL lignin residues was estimated by GPC, and the changes in the lignin depolymerization products during depolymerization with the PTA catalyst were elucidated

(Figure 8c). It was found that the molecular weight of the EL and TL lignin residues was always less than that of the BL. Changes in the molecular weight of these EL and TL lignin residues can affect lignin depolymerization and repolymerization during the reaction. This means that PTA can efficiently catalyze the aryl ether linkages in lignin to form various lignin fragments. In short, the effects of PTA catalysts accelerate lignin depolymerization. In addition, lignin macromolecules were degraded into small molecules with a sharp drop in molecular weight. The TL's molecular weight content is higher than the EL's molecular weight content, which means that the PTA-based catalytic depolymerization process can not only produce aromatic oligomers but also produce repolymerization reactions. Figure 8d shows the atomic ratio results of H/C and O/C for the EL and TL obtained after catalytic depolymerization. Compared to BL, the O/C of all lignin residue samples increased and the H/C of all residue lignin samples decreased after ethanol/water depolymerization. This result indicates that the lignin residue samples obtained during catalysis by PTA might break a large number of side-chain alkane functional molecules [36]. Therefore, lignin residue samples have a small amount of carbon, resulting in a large O/C ratio. In addition, the oxygen content in the TL residue was less than that in the EL residue because a large number of condensation reactions occurred in the TL residue and a new C–C bond could be formed [21]. These results are also consistent with the results of the 2D-HSQC spectra and the GPC analysis in our study. Lignin can be catalyzed efficiently by PTA to form phenolic monomers and small lignin fragments.

3. Materials and Methods

All chemicals and solvents used in this research were of analytical reagent grade and were directly used without purification. PTA, phosphomolybdic acid (PMA), tungstosilicic acid (TSA), dimethyl sulfoxide (DMSO), hydrogen peroxide (H_2O_2), tetrahydrofuran (THF), and ethanol were supplied by Sinopharm chemical reagent Co. Ltd. (Shanghai, China) Standard samples of N-tetradecane, hydrochloric acid (HCl), and ethyl acetate (EAC) were purchased from Aladdin chemical reagent Co. Ltd (Shanghai, China). Lignin was obtained from the pulping of bulrush using the organosolv technique. The lignin model compound was purchased from Macklin Biochemical Co., Ltd (Shanghai, China).

Bulrush lignin (BL) was extracted using the organosolv technique [38]. Eighty grams (80 g) of bulrush residue was added to 800 mL of ethanol/water (*v/v*, 480 mL/320 mL) and heated at 205 °C for 70 min. The mixture was cooled, filtered, and washed with solvent (ethanol/water). The ethanol/water-soluble portion was poured into 5000 mL of hydrochloric acid water solution (pH = 2.0) in order to precipitate lignin. The lignin was then freeze-dried to obtain a dark brown solid.

Catalytic depolymerization experiments were conducted in a 50 mL Parr reactor. Typically, lignin model compound (0.05 g), PTA catalyst (0.025 g), H_2O_2 (0.3 mL), and ethanol/water (*v/v*, 3 mL/3 mL) were combined. The mixture was stirred in the reactor at 250 °C for 6 h. After the reaction, the ethanol was evaporated, 250 mL hydrochloric acid water solution was added, and the reaction solution was adjusted to pH = 2.0. Finally, products were extracted using ethyl acetate.

Catalytic depolymerization experiments were also conducted in a 100 mL Parr reactor. Typically, lignin (0.5 g), PTA catalyst (0.25 g), H_2O_2 (3 mL), and ethanol/water (*v/v*, 30 mL/30 mL) were combined. The mixture was stirred under different reaction conditions. When the desired conditions were reached, the reaction was quenched using water. Yellow and black solids were observed at the bottom of the container. A workup procedure was developed to distinguish the liquid products from the solid residue as shown in Scheme 1. Firstly, the reaction mixture was centrifuged to separate the solid residue and liquid products. Then, the liquid products were acidified to pH = 2.0 and centrifuged to separate water-soluble and water-insoluble samples. Extraction of water-soluble samples was accomplished with EAC. An aliquot of 1 mL was taken and directly analyzed by GC–MS. The water-insoluble samples were referred to as oligomers (an ethanol-soluble lignin residue). At last, the previously obtained solid residue was washed with excess THF. The mixture solution was filtered. The filter cake was retrieved and regarded as bio-char. The THF was removed by rotary evaporation from the THF filtrate, and

unconverted lignin and repolymerized lignin fragments were obtained as a polymer (a THF-soluble lignin residue).
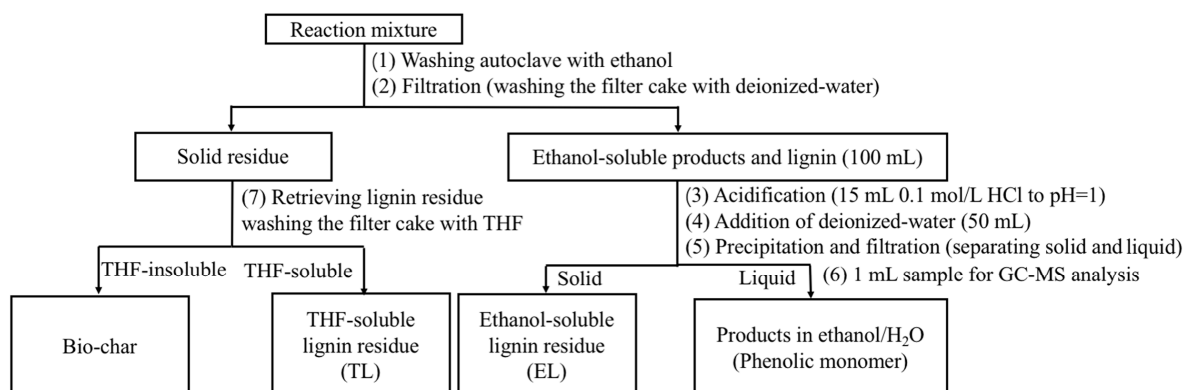
Scheme 1. The workup procedure.

All samples were used without further treatment. The molecular weights of lignin samples were determined by GPC. Analyses were carried out at 25 °C using THF as an eluent with a flow rate of 1 mL/min. For the lignin sample analysis, the sample was prepared at a concentration of 10 mg/mL. All samples were filtered using a 0.45 μm filter membrane prior to injection [39]. The contents of C, H, N, and O were analyzed using a Vario EL III elemental analyzer (Hanau, Germany) [40]. FT–IR analysis was performed using a PerkinElmer spectrum in the wavenumber region from 400 cm^{-1} to 4000 cm^{-1} [24]. The thermal stability analyses were carried out on a thermal stability (TGA) Q500 thermal analyzer (TGA Instruments, USA) by heating the samples from 30 to 700 °C with a 10 °C min^{-1} increment under a nitrogen atmosphere [27]. All prepared lignin samples were dissolved in DMSO-d6. The 2D-HSQC NMR determinations were carried out in a Bruker AVIII 400 MHz spectrometer (Bruker AVANCE NEO, Beijing, China) as reported earlier [41,42]. 2D-HSQC NMR cross-peaks were assigned by combining the results and comparing them with literature results [43,44]. A semi-quantitative analysis of 2D-HSQC NMR cross-peak intensities was performed in the aliphatic oxygenated region. Interunit linkages were estimated from Cα–Hα correlations, and the relative abundance of side chains involved in interunit linkages was calculated [45]. The volume integration of peaks in 2D-HSQC NMR plots was accomplished using Bruker's TopSpin 3.0 software (Bruker AVANCE NEO, Beijing, China). The monomer products were performed using an Agilent 5977A gas chromatography–mass spectrometry (GC–MS) system equipped with a capillary column (30 m × 250 μm × 0.25 μm) and a gas chromatography–flame ionization detector (GC–FID) together with a mass spectrometer detector. The quantitative analyses of the liquid phase product were based on 1 mL GC–FID with N-tetradecane as an internal standard. The FID response factors were calculated using the effective carbon number (ECN) method to determine the relative response factors, which were corrected by the molecular weight of the compounds relative to N-tetradecane [20]. The monomer, lignin residue, and char yields (in wt %) were calculated according to Equations (1)–(4):

$$\text{Yield of phenol monomers (wt \%)} = (WPM/WBL) \times 100\% \tag{1}$$

$$\text{Yield of ethanol-dissolved lignin residue (wt \%)} = (WEL/WBL) \times 100\% \tag{2}$$

$$\text{Yield of THF-dissolved lignin residue (wt \%)} = (WTL/WBL) \times 100\% \tag{3}$$

$$\text{Yield of char residue (wt \%)} = (WC/WBL) \times 100\% \tag{4}$$

In Equations (1)–(4), WBL is the weight of untreated lignin, WEL is the weight of the ethanol-dissolved lignin residue, WTL is the weight of the THF-dissolved lignin residue, WC is

the weight of the bio-char, and WPM is the weight of the phenolic monomer, which was determined by GC–FID.

4. Conclusions

In this work, we have described the effective catalytic depolymerization of BL by the PTA polyoxometallate under relatively mild reaction conditions, selectively furnishing 4-ethylphenol and 4-ethyl-2-methoxyphenol as major phenolic monomer products. High-yield conversion production was developed in ethanol/water using a PTA catalyst at different reaction temperatures and reaction times with little formation of bio-char. The phenolic monomers that were produced after lignin depolymerization may have application in the pharmaceutical field and food industries as platform chemicals [46]. This process would not only help to achieve sustainability goals but also protect the environment. Our method did not require precious metals and harsh reaction conditions—it only required relatively mild reaction conditions and homogeneous catalysis—thereby greatly reducing operating costs and increasing the yields. Therefore, this PTA catalyst, with excellent activity and selectivity in bulrush lignin catalysis, would be a good alternative to the traditional catalysts used in lignin depolymerization and could find wide application in biomass use.

Author Contributions: Conceptualization, investigation, and supervision: X.W., B.L., and J.Z.; proposed methodology and supervision: B.D. and X.W.; validation, formal analysis, and writing: B.D. and Y.Y.

References

1. Kai, D.; Tan, M.J.; Chee, P.L.; Chua, Y.K.; Yap, Y.L.; Loh, X.J. Towards lignin-based functional materials in a sustainable world. *Green Chem.* **2016**, *18*, 1175–1200. [CrossRef]

2. Liu, C.; Hu, J.; Zhang, H.; Xiao, R. Thermal conversion of lignin to phenols: Relevance between chemical structure and pyrolysis behaviors. *Fuel* **2016**, *182*, 864–870. [CrossRef]

3. Azadi, P.; Inderwildi, O.R.; Farnood, R.; King, D.A. Liquid fuels, hydrogen and chemicals from lignin: A critical review. *Renew. Sustain. Energy Rev.* **2013**, *21*, 506–523. [CrossRef]

4. Rinaldi, R.; Jastrzebski, R.; Clough, M.T.; Ralph, J.; Kennema, M.; Bruijnincx, P.C.; Weckhuysen, B.M. Paving the Way for Lignin Valorisation: Recent Advances in Bioengineering, Biorefining and Catalysis. *Angew. Chem. Int. Ed.* **2016**, *55*, 8164–8215. [CrossRef] [PubMed]

5. Ye, Y.; Zhang, Y.; Fan, J.; Chang, J. Selective production of 4-ethylphenolics from lignin via mild hydrogenolysis. *Bioresour. Technol.* **2012**, *118*, 648–651. [CrossRef] [PubMed]

6. Liu, H.; Chung, H. Lignin-based polymers via graft copolymerization. *J. Polym. Sci. Part A Polym. Chem.* **2017**, *55*, 3515–3528. [CrossRef]

7. Bruijnincx, P.C.; Weckhuysen, B.M. Shale gas revolution: An opportunity for the production of biobased chemicals? *Angew. Chem. Int. Ed.* **2013**, *52*, 11980–11987. [CrossRef] [PubMed]

8. Zakzeski, J.; Bruijnincx, P.C.; Jongerius, A.L.; Weckhuysen, B.M. The catalytic valorization of lignin for the production of renewable chemicals. *Chem. Rev.* **2010**, *110*, 3552–3599. [CrossRef]

9. Mahmood, N.; Yuan, Z.; Schmidt, J.; Xu, C.C. Hydrolytic depolymerization of hydrolysis lignin: Effects of catalysts and solvents. *Bioresour. Technol.* **2015**, *190*, 416–419. [CrossRef]

10. Ahmadi, S.; Yuan, Z.; Rohani, S.; Xu, C. Effects of nano-structured CoMo catalysts on hydrodeoxygenation of fast pyrolysis oil in supercritical ethanol. *Catal. Today* **2016**, *269*, 182–194. [CrossRef]

11. Klein, I.; Saha, B.; Abu-Omar, M.M. Lignin depolymerization over Ni/C catalyst in methanol, a continuation: Effect of substrate and catalyst loading. *Catal. Sci. Technol.* **2015**, *5*, 3242–3245. [CrossRef]

12. Güvenatam, B.; Heeres, E.H.J.; Pidko, E.A.; Hensen, E.J.M. Lewis acid-catalyzed depolymerization of soda lignin in supercritical ethanol/water mixtures. *Catal. Today* **2016**, *269*, 9–20. [CrossRef]

13. Agarwal, A.; Rana, M.; Park, J.-H. Advancement in technologies for the depolymerization of lignin. *Fuel Process. Technol.* **2018**, *181*, 115–132. [CrossRef]

14. Renders, T.; Schutyser, W.; Van den Bosch, S.; Koelewijn, S.-F.; Vangeel, T.; Courtin, C.M.; Sels, B.F. Influence of Acidic (H_3PO_4) and Alkaline (NaOH) Additives on the Catalytic Reductive Fractionation of Lignocellulose. *ACS Catal.* **2016**, *6*, 2055–2066. [CrossRef]

15. Yang, H.; Norinaga, K.; Li, J.; Zhu, W.; Wang, H. Effects of HZSM-5 on volatile products obtained from the fast pyrolysis of lignin and model compounds. *Fuel Process. Technol.* **2018**, *181*, 207–214. [CrossRef]

16. Voitl, T.; Rohr, P.R.v. Oxidation of Lignin Using Aqueous Polyoxometalates in the Presence of Alcohols. *ChemSusChem* **2008**, *1*, 763–769. [CrossRef]

17. Deng, H.; Lin, L.; Sun, Y.; Pang, C.; Zhuang, J.; Ouyang, P.; Li, Z.; Liu, S. Perovskite-type Oxide $LaMnO_3$: An Efficient and Recyclable Heterogeneous Catalyst for the Wet Aerobic Oxidation of Lignin to Aromatic Aldehydes. *Catal. Lett.* **2008**, *126*, 106–111. [CrossRef]

18. Xu, W.; Li, X.; Shi, J. Oxidative Depolymerization of Cellulolytic Enzyme Lignin over Silicotungvanadium Polyoxometalates. *Polymers* **2019**, *11*, 564. [CrossRef]

19. Demesa, A.G.; Laari, A.; Sillanpää, M.; Koiranen, T. Valorization of Lignin by Partial Wet Oxidation Using Sustainable Heteropoly Acid Catalysts. *Molecules* **2017**, *22*, 1625. [CrossRef]

20. Xiao, L.P.; Wang, S.; Li, H.; Li, Z.; Shi, Z.; Xiao, L.; Sun, R.; Fang, Y.; Song, G. Catalytic Hydrogenolysis of Lignins into Phenolic Compounds over Carbon Nanotube Supported Molybdenum Oxide. *ACS Catal.* **2017**, *7*, 7535–7542. [CrossRef]

21. Liu, C.; Wang, X.; Lin, F.; Zhang, H.; Xiao, R. Structural elucidation of industrial bioethanol residual lignin from corn stalk: A potential source of vinyl phenolics. *Fuel Process. Technol.* **2018**, *169*, 50–57. [CrossRef]

22. Huang, X.; Gonzalez, O.M.M.; Zhu, J.; Korányi, T.I.; Boot, M.D.; Hensen, E.J. Reductive fractionation of woody biomass into lignin monomers and cellulose by tandem metal triflate and Pd/C catalysis. *Green Chem.* **2017**, *19*, 175–187. [CrossRef]

23. Sun, Y.-C.; Wang, M.; Sun, R.-C. Toward an understanding of inhomogeneities in structure of lignin in green solvents biorefinery. Part 1: Fractionation and characterization of lignin. *ACS Sustain. Chem. Eng.* **2015**, *3*, 2443–2451. [CrossRef]

24. Dai, Z.; Shi, X.; Liu, H.; Li, H.; Han, Y.; Zhou, J. High-strength lignin-based carbon fibers via a low-energy method. *RSC Adv.* **2018**, *8*, 1218–1224. [CrossRef]

25. Huang, X.; Koranyi, T.I.; Boot, M.D.; Hensen, E.J. Catalytic depolymerization of lignin in supercritical ethanol. *ChemSusChem* **2014**, *7*, 2276–2288. [CrossRef]

26. Güvenatam, B.; Heeres, E.H.J.; Pidko, E.A.; Hensen, E.J.M. Lewis-acid catalyzed depolymerization of Protobind lignin in supercritical water and ethanol. *Catal. Today* **2015**, *259*, 460–466. [CrossRef]

27. Wang, X.; Du, B.; Pu, L.; Guo, Y.; Li, H.; Zhou, J. Effect of particle size of HZSM-5 zeolite on the catalytic depolymerization of organosolv lignin to phenols. *J. Anal. Appl. Pyrolysis* **2018**, *129*, 13–20. [CrossRef]

28. Ma, H.; Li, H.; Zhao, W.; Li, L.; Liu, S.; Long, J.; Li, X. Selective depolymerization of lignin catalyzed by nickel supported on zirconium phosphate. *Green Chem.* **2019**. [CrossRef]

29. Asawaworarit, P.; Daorattanachai, P.; Laosiripojana, W.; Sakdaronnarong, C.; Shotipruk, A.; Laosiripojana, N. Catalytic depolymerization of organosolv lignin from bagasse by carbonaceous solid acids derived from hydrothermal of lignocellulosic compounds. *Chem. Eng. J.* **2019**, *356*, 461–471. [CrossRef]

30. Zhao, Y.; Xu, Q.; Pan, T.; Zuo, Y.; Fu, Y.; Guo, Q.-X. Depolymerization of lignin by catalytic oxidation with aqueous polyoxometalates. *Appl. Catal. A Gen.* **2013**, *467*, 504–508. [CrossRef]

31. Ito, H.; Imai, T.; Lundquist, K.; Yokoyama, T.; Matsumoto, Y. Revisiting the Mechanism of β-O-4 Bond Cleavage During Acidolysis of Lignin. Part 3: Search for the Rate-Determining Step of a Non-Phenolic C6-C3 Type Model Compound. *J. Wood Chem. Technol.* **2011**, *31*, 172–182. [CrossRef]

32. Imai, T.; Yokoyama, T.; Matsumoto, Y. Revisiting the mechanism of β-O-4 bond cleavage during acidolysis of lignin IV: Dependence of acidolysis reaction on the type of acid. *J. Wood Sci.* **2011**, *57*, 219–225. [CrossRef]

33. Liao, Y.; d'Halluin, M.; Makshina, E.; Verboekend, D.; Sels, B.F. Shape selectivity vapor-phase conversion of lignin-derived 4-ethylphenol to phenol and ethylene over acidic aluminosilicates: Impact of acid properties and pore constraint. *Appl. Catal. B Environ.* **2018**, *234*, 117–129. [CrossRef]

34. Das, J.; Halgeri, A.B. Selective synthesis of para-ethylphenol over pore size tailored zeolite. *Appl. Catal. A Gen.* **2000**, *194*, 359–363. [CrossRef]

35. Wang, S.; Gao, W.; Li, H.; Xiao, L.P.; Sun, R.C.; Song, G. Selective Fragmentation of Biorefinery Corncob Lignin into p-Hydroxycinnamic Esters with a Supported $ZnMoO_4$ Catalyst. *ChemSusChem* **2018**. [CrossRef]

36. Huang, X.; Korányi, T.I.; Boot, M.D.; Hensen, E.J.M. Ethanol as capping agent and formaldehyde scavenger for efficient depolymerization of lignin to aromatics. *Green Chem.* **2015**, *17*, 4941–4950. [CrossRef]

37. Shen, X.-J.; Wang, B.; Pan-li, H.; Wen, J.-L.; Sun, R.-C. Understanding the structural changes and depolymerization of Eucalyptus lignin under mild conditions in aqueous $AlCl_3$. *RSC Adv.* **2016**, *6*, 45315–45325. [CrossRef]

38. Guo, Y.; Zhou, J.; Wen, J.; Sun, G.; Sun, Y. Structural transformations of triploid of Populus tomentosa Carr. lignin during auto-catalyzed ethanol organosolv pretreatment. *Ind. Crops Prod.* **2015**, *76*, 522–529. [CrossRef]

39. Wang, X.; Guo, Y.; Zhou, J.; Sun, G. Structural changes of poplar wood lignin after supercritical pretreatment using carbon dioxide and ethanol–water as co-solvents. *RSC Adv.* **2017**, *7*, 8314–8322. [CrossRef]

40. Gao, S.; Zhao, J.; Wang, X.; Guo, Y.; Han, Y.; Zhou, J. Lignin Structure and Solvent Effects on the Selective Removal of Condensed Units and Enrichment of S-Type Lignin. *Polymers* **2018**, *10*, 967. [CrossRef]

41. Xiao, L.-P.; Lin, Z.; Peng, W.-X.; Yuan, T.-Q.; Xu, F.; Li, N.-C.; Tao, Q.-S.; Xiang, H.; Sun, R.-C. Unraveling the structural characteristics of lignin in hydrothermal pretreated fibers and manufactured binderless boards fromEucalyptus grandis. *Sustain. Chem. Process.* **2014**, *2*, 9. [CrossRef]

42. Xiao, L.P.; Bai, Y.Y.; Shi, Z.J.; Lu, Q.; Sun, R.-C. Influence of alkaline hydrothermal pretreatment on shrub wood Tamarix ramosissima: Characteristics of degraded lignin. *Biomass Bioenergy* **2014**, *68*, 82–94. [CrossRef]

43. Kim, H.; Ralph, J.; Akiyama, T. Solution-state 2D NMR of ball-milled plant cell wall gels in DMSO-d6/pyridine-d5. *Bioenergy Res.* **2010**, *8*, 576–591. [CrossRef]

44. Mansfield, S.D.; Kim, H.; Lu, F.; Ralph, J. Whole plant cell wall characterization using solution-state 2D NMR. *Nat. Protoc.* **2012**, *7*, 1579–1589. [CrossRef]

45. Wen, J.L.; Sun, S.L.; Xue, B.L.; Sun, R.-C. Recent Advances in Characterization of Lignin Polymer by Solution-State Nuclear Magnetic Resonance (NMR) Methodology. *Materials* **2013**, *6*, 359–391. [CrossRef]

46. Vardon, D.R.; Franden, M.A.; Johnson, C.W.; Karp, E.M.; Guarnieri, M.T.; Linger, J.G.; Salm, M.J.; Strathmann, T.J.; Beckham, G.T. Adipic acid production from lignin. *Energy Environ. Sci.* **2015**, *8*, 617–628. [CrossRef]